PROCEEDINGS, 48th Workshop on Geothermal Reservoir Engineering
Stanford University, Stanford, California, February 6-8, 2023
SGP-TR-224

Shut-In Testing on the 4100L - Implications on the State of Stress, Fractures, and Wellbores in the Second EGS Collab Testbed

Paul Schwering[1], Mathew Ingraham[1], Vince Vermeul[2], Jeff Burghardt[2], Tim Johnson[2], Chris Strickland[2], Mark White[2], Chet Hopp[3], Verónica Rodríguez Tribaldos[3], Tim Kneafsey[3], Tyler Artz[4], Earl Mattson[5], Thomas Doe[6], and the EGS Collab Team*

[1]Sandia National Laboratories, Albuquerque, New Mexico, USA

[2]Pacific Northwest National Laboratory, Richland, Washington, USA

[3]Lawrence Berkeley National Laboratory, Berkeley, California, USA

[4]RESPEC Company LLC, Rapid City, South Dakota, USA

[5]Mattson Hydrology LLC, Victor, Idaho, USA

[6]TDoe Geo, Redmond, Washington, USA

pcschwe@sandia.gov

Keywords: enhanced geothermal system, instantaneous shut-in pressure, distributed fiber, fracture network, minimum principal stress

ABSTRACT

In the summer of 2022, the EGS Collab Project conducted a 2-month long multi-well hydraulic circulation test in the 4100L drift of the Sanford Underground Research Facility. This circulation test was conducted in a fracture network that had previously been hydraulically stimulated in the Yates Amphibolite crystalline rock formation hosting the second EGS Collab testbed. The cross-well injection and production of water was continuously conducted and measured using an instrumented network of downhole straddle packers which were operated through a flow and pressure-controlled hydraulic injection system. Onsite observers and an array of downhole geophysical monitoring systems recorded crucial data to supplement the hydraulic pressure and flow measurements from the injection control system. EGS Collab Team members executed a series of shut-in tests during the final days leading up to, and upon, the conclusion of the hydraulic circulation test. The purpose of this paper is to present the results and findings from the shut-in testing by describing 1) the primary motivations for conducting the tests; 2) the instrument configuration leading up to and through the shut-in tests; 3) the shut-in execution sequence and technical challenges; 4) data collected from the hydraulic injection control system, geophysical monitoring arrays, and on-site personnel on the 4100L; and, 5) interpretations and lessons/implications from this shut-in series.

Shut-in tests are routinely conducted to assess fracture closure and evaluate in-situ stress parameters of the rock formation. In a multi-zone test bed, the pressure responses also provide information on connectivity of the injection zone to monitored intervals. By conducting shut-in testing after hydraulic stimulation and circulation, phenomena such as local stresses and near-wellbore interactions (i.e., skin effects) can also be examined. Analyses of the shut-in tests add crucial technical context specific to the EGS Collab experiment and have more broad implications to larger-scale applications in relevant conditions (e.g., commercial-scale EGS in crystalline rock). Straddle packers were deployed in four subhorizontal wells - one injector and three producers - at various depths.

The two-month long injection was conducted at a rate of 3.4 liters per minute at a nearly steady injection pressure of over 30 MPa (approximately 4,400 psi). During that time, the intervals in the producing boreholes were open to atmospheric pressure. The production flow rates from short, targeted intervals, as well as the borehole sections above and below those intervals, were monitored continuously for outflow. Production rates in the wells ranged from 10's to 100's of mL per minute. Significant water production was also measured from multiple locations in the 4100L drift. The rates and locations of outflow varied over time.

*J. Ajo-Franklin, T. Artz, T. Baumgartner, K. Beckers, G. Bettin, D. Blankenship, A. Bonneville, L. Boyd, S. Brown, J.A. Burghardt, C. Chai, A. Chakravarty, T. Chen, Y. Chen, B. Chi, K. Condon, P.J. Cook, D. Crandall, N. Creasy, R. DeBoer, P.F. Dobson, T. Doe, C.A. Doughty, D. Elsworth, J. Feldman, Z. Feng, A. Foris, L.P. Frash, Z. Frone, P. Fu, K. Gao, A. Ghassemi, Y. Guglielmi, B. Haimson, A. Hawkins, J. Heise, C. Hopp, M. Horn, R.N. Horne, J. Horner, M. Hu, H. Huang, L. Huang, K.J. Im, M. Ingraham, E. Jafarov, R.S. Jayne, T.C. Johnson, S.E. Johnson, B. Johnston, S. Karra, K. Kim, D.K. King, T. Kneafsey, H. Knox, J. Knox, D. Kumar, K. Kutun, M. Lee, D. Li, J. Li, K. Li, Z. Li, M. Maceira, P. Mackey, N. Makedonska, C.J. Marone, E. Mattson, M.W. McClure, J. McLennan, T. McLing, C. Medler, R.J. Mellors, E. Metcalfe, J. Miskimins, J. Moore, C.E. Morency, J.P. Morris, T. Myers, S. Nakagawa, G. Neupane, G. Newman, A. Nieto, T. Paronish, R Pawar, P. Petrov, B. Pietzyk, M. Plummer, R. Podgorney, Y. Polsky, J. Pope, S. Porse, J.C. Primo, T. Pyatina, J. Quintanar, C. Reimers, B.Q. Roberts, M. Robertson, V. Rodríguez Tribaldos, W. Roggenthen, J. Rutqvist, D. Rynders, M. Schoenball, P. Schwering, V. Sesetty, C.S. Sherman, A. Singh, D. Sirota, M.M. Smith, H. Sone, E.L. Sonnenthal, F.A. Soom, D.P. Sprinkle, S. Sprinkle, J. St. Clair, C.E. Strickland, J. Su, Y. Tanaka, N. Taverna, D. Templeton, J.N. Thomle, C. Ulrich, N. Uzunlar, A. Vachaparampil, C.A. Valladao, W. Vandermeer, G. Vandine, D. Vardiman, V.R. Vermeul, J.L. Wagoner, H.F. Wang, J. Weers, N. Welch, J. White, M.D. White, P. Winterfeld, T. Wood, S. Workman, H. Wu, Y.S. Wu, E.C. Yildirim, Y. Zhang, Y.Q. Zhang, Q. Zhou, M.D. Zoback

Shut-in testing was conducted in two stages. The first stage involved closing seven production zones (straddle packer intervals and bottom zones) while maintaining the 3.4 liter per minute rate in the injection well. This shut-in stage provided information on the pressures in the isolated production intervals. Once all production zones were shut-in, injection continued for another 24 hours before initiating a second shut-in stage in which injection was stopped and the injection interval was shut-in to monitor pressure decay. Pressure decay responses generally indicate that the stimulated fracture network had an average residual pressure of approximately 20 MPa, in agreement with minimum principal stress estimates obtained in a nearby borehole. Observed evolution of the outflow system in the wells and the drift indicates a dynamic, interconnected fracture network throughout the testbed. Geophysical monitoring data were recorded during the shut-in sequence, which provided additional insights on the timing and spatial distribution of flow propagation, changes in stress, and fracture relaxation.

1. INTRODUCTION

The primary goal of the EGS Collab project is to refine the collective understanding of rock mass response to stimulation for the purpose of enabling enhanced geothermal system (EGS) energy utilization. Understanding and predicting permeability enhancement and evolution in crystalline rock is key to EGS commercialization. The ability to target and produce distributed permeability for heat extraction from a reservoir, via generating new fractures that complement existing fractures, will reduce the financial risk of EGS. Towards this end, experiments on the 10-meter scale (i.e., mesoscale) were performed in crystalline rock under stresses relevant to EGS. Tests and analyses were performed to support improvement and validation of thermal-hydrological-mechanical-chemical (THMC) modeling approaches. In addition, conventional and novel field monitoring tools were tested and improved. Three multi-test experiments were performed to increase understanding of stimulation methods: hydraulic fracturing (Experiment 1), shear stimulation (Experiment 2), and other stimulation methods (Experiment 3). To build confidence in methodology and improve the array of stimulation and monitoring tools in use, modeling/simulation directly supported experiment design and execution. Computational analyses were performed for model validation, examining the effectiveness of instrumentation and deployment strategies, and to explain field observations.

1.1 Background

EGS Collab experiments were performed at the Sanford Underground Research Facility (SURF) located in Lead, South Dakota (Heise, 2015). The Experiment 2 testbed is located in the 4100L drift at approximately 1.25 km depth (i.e., a horizontal mine tunnel approximately 4,100 feet below the ground surface) in the Yates amphibolite. The Yates amphibolite is a blocky, low permeability rock. Subsurface stress and lithologic conditions are different from those of the preceding kISMET and Experiment 1 tests, which were performed in the 4850L drift at approximately 1.5 km depth in the Poorman phyllite/schist (Oldenburg et al., 2017; Kneafsey et al., 2020).

EGS Collab Experiment 1 comprised three primary stages: 1) hydraulic fracture stimulation, 2) chilled-water circulation, and 3) shut-in. The stimulation stage yielded a fracture network of both hydraulically induced and natural fractures. Fracture stimulation from a straddle packer interval in the injection well successfully achieved hydraulic connection to the target production well, and this configuration was selected for a chilled-water circulation test (Kneafsey et al., 2020). The chilled-water circulation test was started on 08 May 2019 and continued for 196 days. Except for occasional outages, chilled water was injected at a constant rate of 0.4 liters per minute (L/min), a rate that did not result in additional micro-seismicity, indicating a stable hydraulic fracture extent. The chilled water circulation experiment yield three scientifically interesting responses: 1) nearly instantaneous drop in injection pressure when injection switched from ambient temperature water to chilled water, 2) sharp drop in injection pressure following each injection cessation, and 3) a steady gradual increase in flow resistance across the fracture network over time (White & Burghardt, 2021). Most of the experiment time and focus was dedicated to these stimulation and circulation stages.

A relatively short shut-in stage at the conclusion of the chilled-water circulation test provided valuable information about characteristics of the fracture network. The generally accepted conceptual model for the fracture network connecting the injection and production wells during the chilled-water circulation test was that water entered a hydraulic fracture from the injection interval, which incurred flow resistance at that intersection, and the injected water was transmitted to the production well along two pathways: a) directly via a hydraulic fracture that connected with the production well and b) indirectly via an intersection with a natural fracture that also intersected the production well at a shallower depth than the direct pathway. Flow and pressure measurements throughout the course of the chilled-water experiment were supplemented with tracer tests (Neupane et al., 2020). This generated valuable data against which numerical simulations could be benchmarked and provided insights to the behavior of the mesoscale EGS reservoir.

The steady nature of the chilled-water circulation test, however, did not provide details about the specifics of the inter-fracture and fracture-borehole connections. Furthermore, the injection zone was the only point of pressure monitoring, all other production/injection intervals being open to mine air pressure to allow monitoring of outflow. Due to near-borehole effects, the injection-zone pressure is an upper bound to the pressure in the inflated fracture network, and shut-in tests were required to obtain a more accurate value for pressure in that network. Therefore, near the conclusion of the chilled-water circulation test, three different shut-in tests were conducted: 1) shut-in the production well straddle packer interval, 2) shut-in of the zone below the production interval, and then 3) shut-in the whole production well. Shut-in of the interval forced the hydraulic connection to be limited to the hydraulic fracture and yielded higher flow rates than the pre-shut-in values. Shut-in of the bottom zone, likewise, limited the connection through the natural fracture and yielded lower flow rates than the pre-shut-in values. Interestingly, none of the shut-in tests yielded pressure increases in the injection well. Conclusions from these shut-in tests were: 1) pressure in the injection interval is independent of that in the hydraulic fracture, 2) produced water in bottom production zone appears to be dependent on the pressure in the hydraulic fracture (i.e., it's effective permeability is large enough not to impact the flow), 3) the instantaneous shut-in pressure (ISIP) responses indicate that there is a considerable pressure drop between the injection and production wells that may be related to fracture and/or near-wellbore skin effects, 4) there is a flow restriction at/near the injection interval that appears to be insensitive to the mean hydraulic fluid fracture pressure, 5) a flow restriction at the bottom zone of the production well appears to respond to the mean hydraulic

fracture fluid pressure, and 6) the natural fracture pathway is more permeable than the hydraulic fracture pathway per Mattson et al. (2021). Notwithstanding the shut-in tests were of short duration, they provided high-value information about the hydraulic network of Experiment 1. Thus, shut-in testing was prioritized for the next testbed.

The pressures reported in this paper are the values measured at gauges installed at the borehole collars rather than points within the test intervals. The values represent *gauge* pressure and not *absolute* pressure. Minor variations in the mine air pressure due to ventilation in the drift are negligible.

1.2 Testbed Description

Prior to Experiment 2, tests were performed to characterize the nature of shearing in this testbed (Ingraham et al., 2020). Studies suggested reasonable probability to induce shearing (Dobson et al., 2018; Singh et al., 2019; Burghardt et al., 2020; Meng et al., 2021; Meng et al., 2022;). To gain initial information on the testbed, features including fractures and mineralogical changes that were observed along the 4100L drift wall were mapped. Furthermore, a 10 m horizontal borehole (TH4100) and a 50 m vertical borehole (TV4100) were drilled and cored. The vertical borehole TV4100 penetrated a rhyolite layer within the amphibolite. Additional investigations in the drift indicated this to be a gently dipping layer. Hydraulic fracturing stress measurements were performed in TV4100 (Burghardt et al., 2020; Ingraham et al., 2020). Eighteen hydraulic fracturing tests were also performed in TV4100 using the Step-Rate Injection Method for Fracture In-Situ Properties (SIMFIP) tool (Guglielmi et al., 2014; Guglielmi et al., 2015; Guglielmi et al., 2021a; Guglielmi et al., 2021b). Eight of these tests detected components of shear displacement. Stress tests showed significant stress heterogeneity related to the intercepted rhyolite layer. Specifically, the ISIP values above the rhyolite ranged from 20.0 to 22.7 MPa. The average values for the rhyolite and the amphibolite below the rhyolite were 16.5 and 27.8 MPa, respectively (Ingraham et al., 2020). The Experiment 2 test bed was therefore established above the dipping rhyolite layer to avoid this stress heterogeneity (Kneafsey et al., 2022a).

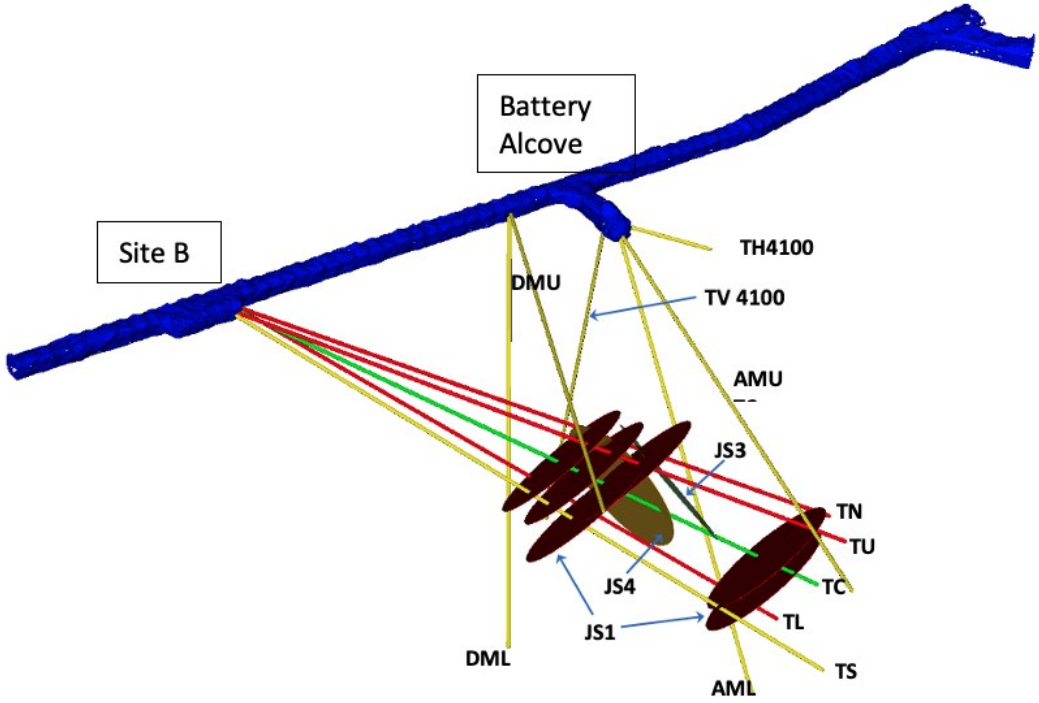

Figure 1: Experiment 2 testbed, oblique view looking downward and to the northwest. Thick blue object = 4100L drift (i.e., horizontal mine tunnel), green line = injection well, red lines = production wells, and yellow lines = monitoring wells. All wells are subhorizontal except for TV4100, which is near vertical. Natural fracture joint set (JS) orientations of wells that connect the injection and production wells are represented by ovals, and hotter colors indicate greater slip tendency. JS1 has a higher slip tendency than other fracture set orientations.

The Experiment 2 testbed comprises nine approximately 10 cm diameter subhorizontal boreholes, ranging from 55 to 80 m deep, which were drilled and cored in 2021 (Figure 1; Table 1). These consisted of two pairs of monitoring wells fanning the test zone. These wells contain grouted sensors and fan out from a location in the Battery Alcove (wells AMU and AML) and a location in the 4100L drift (wells DMU and DML). The other 5 wells consisted of a central well (TC), planned for injection, surrounded by four wells without grouted instrumentation to be used for production and monitoring (wells TU, TL, TN, TS). These wells extend from Site B. The analyses of hydraulic shearing interrogated five joint sets that were observed in wells and the drift (Burghardt et al., 2022). Well TC was optimally oriented to intersect natural fractures that had the highest probability of shear upon stimulation (Kneafsey et al., 2022b). A more detailed description of the Experiment 2 testbed can be found in Kneafsey et al. (2022b).

Table 1: Attributes of the Experiment 2 testbed wells. Tilt refers to angle off horizontal, bearing is referenced to true north.

Well Name	Borehole Length (m)	Tilt (degrees)	Bearing (degrees)	Notes
TH4100	10	-5	45	Initial exploratory corehole.
TV4100	50	-90	N/A	Initial exploratory corehole, initial SIMFIP fracture tests, packed off and monitored during post-stimulation circulation testing.
TC	76	-15	50	Central SIMFIP stimulation well, planned central injection well but was converted to flow production/monitoring well for post-stimulation circulation testing.
TU	76	-8	58	Upper test well, planned flow production/monitoring well but was stimulated and converted to injection well for post-stimulation circulation testing.
TS	80	-16	42	Southern test well for flow production/monitoring.
TN	76	-13	42	Northern test well for flow production/monitoring.
TL	76	-22	48	Lower test well for flow production/monitoring.
AMU	60	-9	101	Upper monitoring alcove well, fully grouted with geophysical instrumentation.
AML	60	-39	100	Lower monitoring alcove well, fully grouted with geophysical instrumentation.
DMU	55	-1	117	Upper monitoring drift well, fully grouted with geophysical instrumentation.
DML	55	-35	123	Lower monitoring drift well, fully grouted with geophysical instrumentation.

1.3 Stimulation and Circulation Experiment Summary

Experiment 2 stimulation tests were conducted in March of 2022 using the SIMFIP tool. A summary of activities is provided in Table 2 below and more details are available in Kneafsey et al. (2023). The conclusion was, despite the many measurements and analyses suggesting a reasonable probability of shear stimulation, that no significant shear-induced fracture permeability was produced from these stimulation tests. That is, the stimulated rock mass did not retain any post-stimulation hydraulic conductivity and thus had to be kept under hydraulic pressure (i.e., "hydro-propped") to maintain permeability. The EGS Collab Team thus proceeded to Experiment 3 stimulations.

Table 2: Timeline and summary of Experiment 2 stimulation activities. All simulations were conducted in well TC using SIMFIP.

Start Time (UTC)	End Time (UTC)	Top of Interval (m)	Bottom of Interval (m)	Notes
3/23/22 14:21	3/23/22 19:28	8.23	10.64	Tensile hydraulic fracture at shallow depth outside of monitoring zone to verify fracture pressure. Hydraulic test was done on 24 March 2022 in the same zone.
3/23/22 21:38	3/24/22 14:38	58.64	61.05	Overnight pressure held at 15.2 MPa (2200 psi).
3/24/22 14:38	3/24/22 17:11	63.46	65.87	60-minute pressure held at 15.2 MPa (2200 psi).
3/24/22 17:12	3/24/22 19:10	53.83	56.24	60-minute pressure held at 15.2 MPa (2200 psi).

3/24/22 19:10	3/24/22 21:04	49.01	51.42	Pressure held at 15.2 MPa (2200 psi). Subsequent injections into TU on 05 May 2022 fractured into this zone and on 06 May 2022 injections were made into the fracture that was created from TU. Additional high-rate injections were made on 18 May 2022. These later injections are documented as part of Experiment 3.
3/24/22 21:04	3/24/22 22:08	44.20	46.61	Pressure held at 15.2 MPa (2200 psi). Subsequent injections in this zone were made on 13 April 2022 and are documented as part of Experiment 3.
3/24/22 22:08	3/24/22 22:42	8.23	10.64	Held pressure at 15.2 MPa (2200 psi) to evaluate post-fracture hydraulic conductivity. The fracture was generated on 23 March 2022 as a tensile fracture.
3/25/22 0:00	3/25/22 0:00	61.05	63.46	Pressure held at 16.1 MPa (2340 psi). Test was shortened to less than 60 minutes due to time constraints.
3/25/22 15:23	3/25/22 17:52	46.60	49.01	Pressure held at 16.1 MPa (2340 psi). There was a Quizix pump communication problem that resulted in a premature depressurization of the interval. The test was resumed but was shortened from the planned 60-minute hold.
3/25/22 17:52	3/25/22 19:21	51.42	53.83	Pressure held at 16.1 MPa (2340 psi). Test was shortened to less than 60 minutes due to time constraints. On 14 April 2022 a stimulation was made in this zone by cycling the injection pressure above/below the fracture opening pressure repeatedly. This later injection is documented as part of Experiment 3.
3/25/22 19:23	3/25/22 20:50	56.23	58.64	Pressure held at 16.1 MPa (2340 psi). Test was shortened to less than 60 minutes due to time constraints.
3/25/22 22:08	4/11/22 17:02	58.64	61.05	Pressure held at 16.1 MPa (2340 psi) from 25 March 2022 until 11 April 2022 to give as much time as possible for pressure to diffuse into natural fractures and promote shear slip/stimulation. On 11 April 2022, after no indication of shear stimulation had occurred, a constant rate injection at 3 mL/min was started. This is considered as the transition to Experiment 3 since the pressure was intentionally allowed to exceed the least compressive principal stress.

Experiment 3 stimulation and flow tests were conducted in April of 2022. A summary of activities is provided in Table 3 below and more details are available in Kneafsey et al. (2023). The SIMFIP tool was initially utilized for a series of tests in TC. Observations and measurements from these tests highlighted a zone in TC that looked suitable for high flow-rate stimulation and flow testing. The SIMFIP tool (2.41 m interval length to accommodate instrumentation) was demobilized. In May of 2022, a straddle packer assembly with a smaller interval length (0.67m) was deployed to more precisely target the TC fracture stimulation zone. Furthermore, a stimulation was conducted in TU to try and promote hydraulic connectivity between TU and TC. A 5 L/min injection into TC resulted in outflows that were largely not captured by the surrounding test wells; outflow appeared to be concentrated downward and towards the 4100L drift. Given these results, the decision was made to stimulate TU instead with the aim of increased injection recovery in the other test wells. On 19 May 2022, one of the two zones stimulated in TU was selected for circulation testing.

Table 3: Timeline and summary of Experiment 3 stimulation activities. Note the transition from SIMFIP to the 26" straddle.

Start Time (UTC)	End Time (UTC)	Top of Interval (m)	Bottom of Interval (m)	Stimulated Well	Injection Straddle	Notes
4/11/22 17:02	4/12/22 19:50	58.64	61.05	TC	SIMFIP	Constant rate injection at increasing rates, then shut-in when fracture was detected in monitoring well AMU via DTS anomaly and dripping from well head. Subsequent flow test, observed with a downhole camera, was conducted on 20 April 2022.

4/12/22 19:52	4/13/22 21:51	44.20	46.61	TC	SIMFIP	Pressure held at 13.8 MPa (2000 psi) overnight. On 14 April 2022 a high-rate injection was conducted and stopped when outflow was observed in the drift.
4/13/22 21:52	4/14/22 15:44	58.64	61.05	TC	SIMFIP	Hydraulic test of fracture created with constant-rate injections on 11-12 April 2022.
4/14/22 15:46	4/14/22 18:15	44.20	46.61	TC	SIMFIP	Hydraulic test of fracture created on 13 April 2022.
4/14/22 18:16	4/18/22 17:35	51.42	53.83	TC	SIMFIP	Cyclical injection above/below fracture pressure until 40 L had been injected and flow from production wells was observed. Following this stimulation, the well was held under 16.1 MPa (2340 psi) constant pressure for several days to observe flowback. Subsequently an injection was made on 21 April 2022 into this zone with the downhole camera deployed in TN and TL to observe outflow locations.
5/5/22 18:39	5/7/22 0:00	54.07	54.74	TU	26" straddle	Initial stimulation of this zone.
5/18/22 14:24	5/19/22 13:52	50.44	51.11	TC	26" straddle	Stimulation at 5 L/min. Outflow was mostly from TL with about 20-25% recovery. Weeps in the drift near the Battery Alcove were observed. Flow was stopped on the evening of 19 May 2022 3:44:55 after an intersection with DML was observed with the DTS.
5/19/22 13:42	5/19/22 13:52	50.44	51.11	TU	26" straddle	Stimulation of this zone, leakage observed at DML.
5/19/22 13:53	8/26/22 20:38	54.07	54.74	TU	26" straddle	Long-term thermal circulation with injection into TU. Both the injection location in TU and the production packer locations in TN, TL, and TU were adjusted to optimize fluid recovery.

The thermal circulation test was conducted by pumping chilled water into the TU injection interval and continuously monitoring the response (Kneafsey et al., 2023; Mattson et al., 2023). The test was interrupted in early June by an injection pump failure, but resumed on 15 June 2023 (Mattson et al., 2023). The injection rate varied somewhat but was kept at 3.4 L/min for the vast majority of the circulation test. Outflow (i.e., injection recovery) locations and rates varied with time, but in general the test wells accounted for approximately 30% of recovery and the drift accounted for the remainder/majority (Mattson et al, 2023). The highest-producing well was TN, which geometrically resides between injection well TU and the drift and accounted for almost all outflow recovered from the test wells. The heavily stimulated well TC, on the other hand, only recovered outflow at rates of a few 10's of mL/min during the entire circulation test. The straddle packer interval in TN was initially only recovering approximately 25% of the total outflow being recovered in TN; the majority was being recovered at the TN well collar, which indicated most of the outflow was above the straddle packer. On 28 July 2022, the TN straddle packer was incrementally moved up-hole by a total of approximately 3.2 meters, while injection continued, until the TN interval straddled the highest-producing zone (Mattson et al., 2023). This augmented configuration changed the bottom, interval, and collar recovery ratios for the TN well to approximately 25%, 75%, and ~0%, respectively, making the TN interval the highest outflow recovery zone of all the test wells. No evidence of thermal breakthrough, however, was detected in any of the test well zones throughout the duration of the circulation test (Mattson et al., 2023). Schedule constraints required bringing the circulation test to a close and transitioning to shut-in testing in August of 2022.

2. SHUT-IN METHODOLOGY

The stimulation and circulation system installed in this testbed was a step-function upgrade in operational sophistication and technological capabilities compared to the Experiment 1 system (Ingraham et al., 2021). The ability to remotely control and measure multiple zones in multiple wells enables robust spatial interrogation of the testbed, improves detection of processes during testing, and allows for greater flexibility in the timing and execution of testing. Furthermore, the testing system provided opportunities to measure pressure within the stimulated fracture network during injection. Consequently, EGS Collab shut-in testing capabilities were drastically improved with this system with the intention of being able to verify consistency and/or heterogeneity in the stimulated fracture network. Furthermore, shut-in tests could be efficiently conducted in multiple locations during or after injection. This priority was recognized from the shut-in data collected during Experiment 1 and was underscored by the stress measurement variations in TV4100 (White & Burghardt, 2021; Ingraham et al., 2020). This approach and technology also allowed for evaluation of near-wellbore skin effects and permeability pathways that would otherwise be very difficult to separate and resolve.

The EGS Collab team sought to leverage the capabilities of this system to conduct shut-in testing in two primary phases. The first phase was shut-in tests of production zones while continuing injection at the circulation test rate (3.4 L/min) with a goal of evaluating how the pressure distribution behaved within the stimulated fracture network during injection. The second phase is a full shut-in test that includes shut-in of the injection zone to investigate hydraulic interactions while the stimulated fracture system returns to equilibrium.

3. TEST SEQUENCE AND OBSERVATIONS

Figure 2 shows a one-month period which captures the entire shut-in test series. The four panels of the plot, from top to bottom, correspond to the TU (injection), TN, TL, and TC wells in which straddle packers are deployed. In each of these wells, hydraulic flow rate is measured from the straddle packer interval (injection or production), the bottom zone below the lower straddle packer, and the outflow of the collar (effectively the zone above the upper straddle packer). Pressure is recorded from the interval and bottom zones (the upper zone being open to atmospheric pressure) in each of the four wells. These eight zones are each utilized and monitored for shut-in testing. Subsequent plots in this section zoom in on individual shut-in test durations while showing these same four panels.

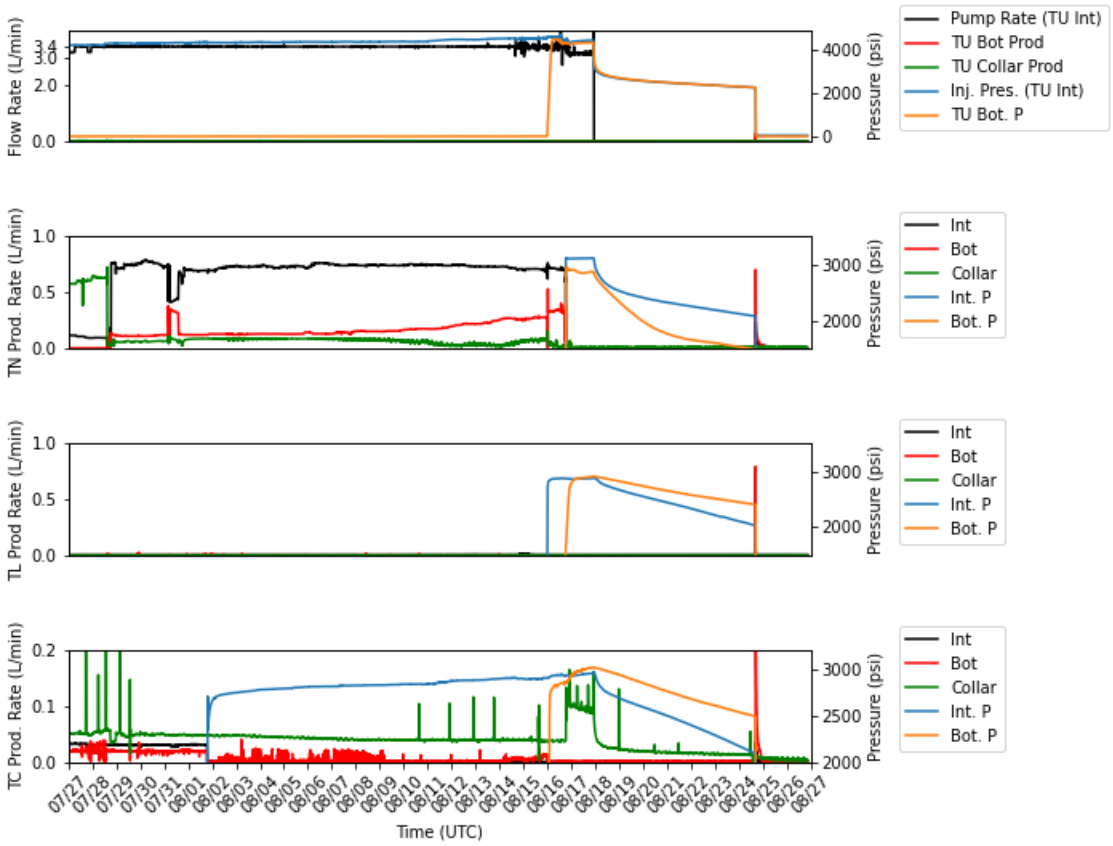

Figure 2: Pressure and flow plots of wells TU, TN, TL, and TC (from top panel to bottom panel) spanning 27 July thru 27 August 2022. For each well, black line = interval zone flow (L/min); red line = bottom zone flow (L/min); green line = well collar outflow (L/min), blue line = interval zone pressure (psi); and, orange line = bottom zone pressure (psi). Events captured in this plot include moving the TN straddle packer on 28 July, the shut-in of the TC interval on 01 August, end of chilled water injection on 10 August, shut-in testing of production zones on 16 August, end of injection and shut-in test of the injection zone on 17 August, and opening all zones on 24 August 2022.

3.1 TC Interval Shut-In Test

The first shut-in test was conducted in the TC interval on 01 August 2022 (Figure 3). This packer interval was selected at this time because, while it provided an opportunity to perform a first, single-zone shut-in test on a producing interval, the interval was only producing approximately 30-40 mL/min (recovering ~1% of injection) and thus would not have a significant impact on the continuing multi-well circulation test. This test begins with a peculiar looking transient/spike in TC interval pressure; this is an artifact related to the interval pressure momentarily exceeding the packer pressure, followed by recovery of the packer pressure and isolation of the interval. The shut-in test then assumed a more typical behavior, with the interval pressure increasing to approximately 18.3 MPa (2,650 psi) by 02 August 2022. The interval pressure continued to slowly increase to approximately 19.0 MPa (2,750 psi).

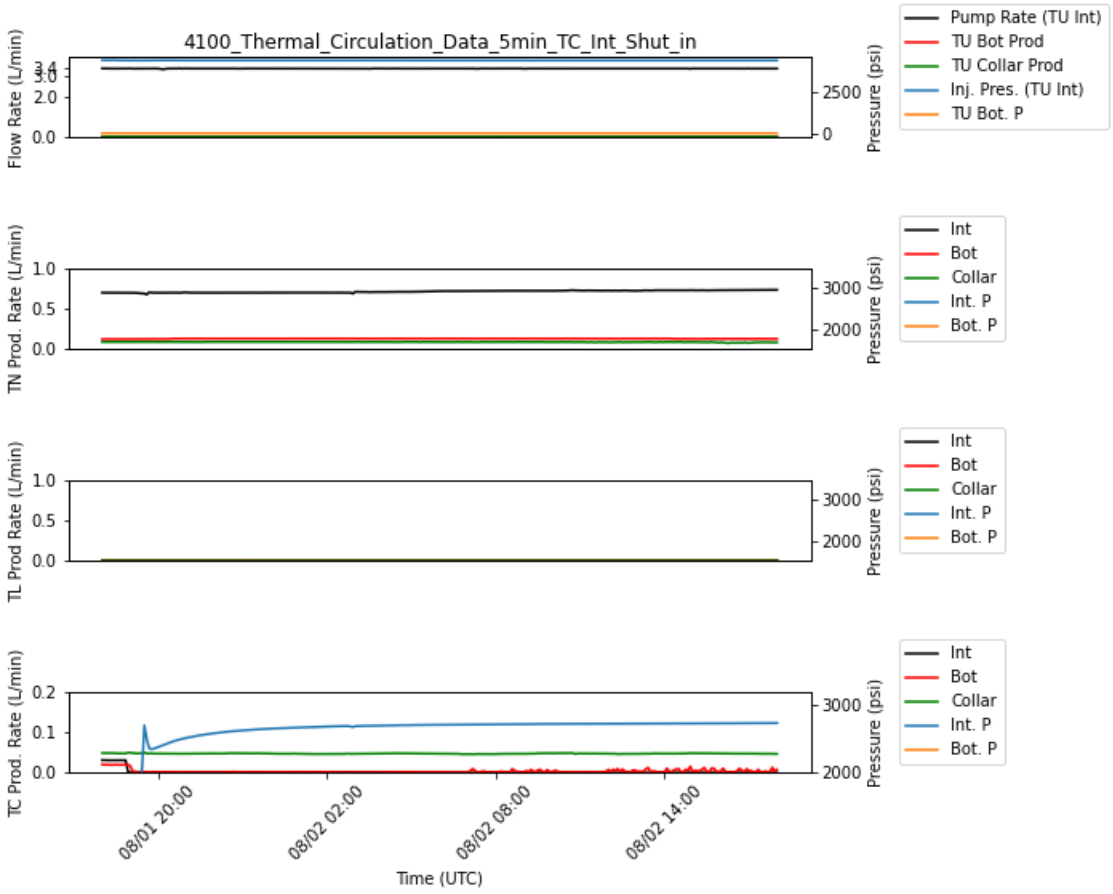

Figure 3: TC interval shut-in test.

On 10 August 2022, the temperature of injection into the TU packer interval was changed from chilled water injection at approximately 13°C to a nominal injection temperature of approximately 21°C. The increased injection temperature was accompanied by a noticeable increase of pressure in the TU injection interval – a phenomenon which was also observed during Experiment 1 (White & Burghardt, 2021). The shut-in pressure of the TC packer interval also increased during this period (Figure 2). By 15 Aug 2022, the pressure in each interval was approximately 31.0 MPa (4,500 psi) and 20.0 MPa (2,900 psi), respectively. Outflow seemed to shift slightly from the TN interval (reduced from approximately 740 to 710 mL/min) to the bottom zone of TN (increased from 180 to 280 mL/min). Observers in the 4100L drift noted that a small portion of the injection recovery seems to also have shifted to the TS well (increase from 0 to 60 mL/min outflow from the well collar), which was instrumented for geophysical monitoring and thus did not contain a straddle packer assembly.

3.2 Multi-Well Shut-In Tests

To start bringing the circulation test to a close, the EGS Collab team elected to begin by shut-in testing of the remaining producing zones that could be controlled with the remote operations system while continuing injection in the TU packer interval. Early on 16 August 2022, shut-in testing was initiated in the TU bottom, TL packer interval, and TC bottom zones (Figure 4). These were three low-production zones, with outflows measuring less than 10 mL/min each prior to shut-in testing. The TU bottom zone increased to approximately 30.3 MPa (4,400 psi), closely matching with the TU injection interval pressure. The TL packer interval quickly reached a stable pressure of approximately 20.0 MPa (2,900 psi). The TC bottom zone initially held at a pressure of 19.6 MPa (2,850 psi), but gradually increased to 20.7 MPa (3,000 psi) through 17 August 2022. The brief interruption in TN outflows during this shut-in sequence are related to an initial attempt to shut-in this well too, but this was quickly abandoned in favor of conducting another three-zone shut-in test later in the day.

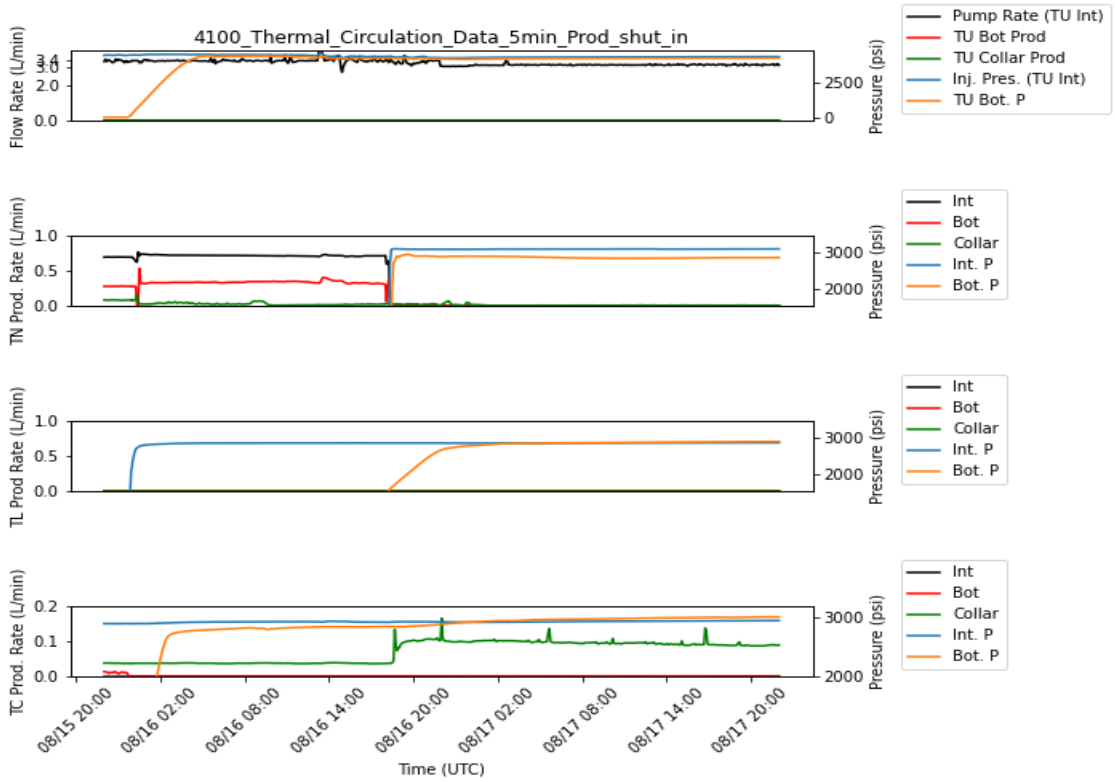

Figure 4: Shut-in tests of multiple production zones during injection.

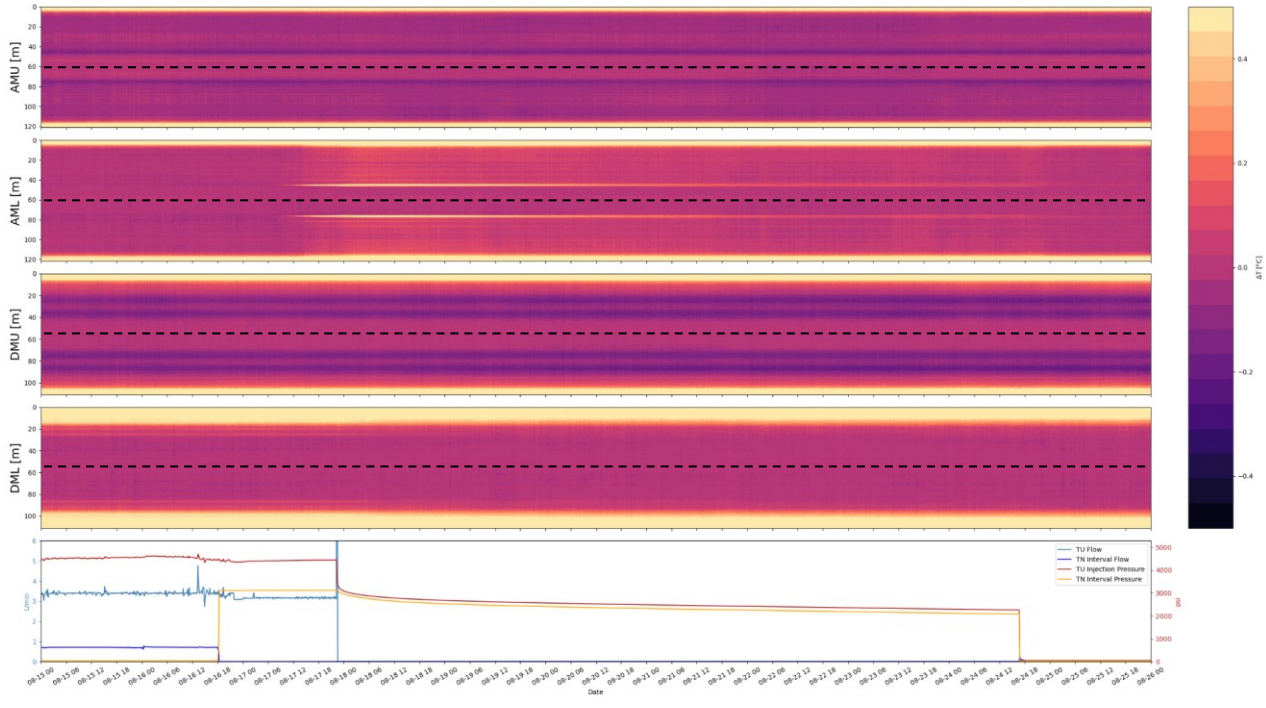

Figure 5: "Waterfall" color plot showing changes in temperature detected by the continuous DTS fiber going down and back up each of the four grouted monitoring wells AMU, AML, DMU, and DML (upper four panels) during shut-in testing (flow/pressure plot for reference in bottom panel). Dashed line indicates the bottom of each well. The time and color saturation scales highlight the AML temperature spike at a downhole depth of approximately 45 meters.

Another three-zone shut-in test, while maintaining injection in the TU interval, was conducted late on 16 August 2022 – the TL bottom zone and the TN bottom and interval zones were all shut-in, thus closing all producing zones that could be shut-in (Figure 4). The low-producing (< 10 mL/min) TL bottom zone, like the TL packer interval, reached a stable pressure of approximately 20.0 MPa (2,900 psi). The high-producing TN zones (combined outflow of ~1 L/min) had slightly different shut-in behaviors. The TN packer interval quickly arrived at a steady pressure of 21.4 MPa (3,100 psi). The bottom zone, however, was less stable initially but reached a steady pressure of approximately 19.7 MPa (2,850 psi). The outflow of the TC collar increased from approximately 70 to 110 mL/min (Figure 4).

Distributed temperature sensing (DTS) detected a distinct temperature change in grouted monitoring well AML after starting this shut-in test. The temperature spike can be seen in Figure 5 at a depth of approximately 45 meters (and again 75 meters on the return portion of the continuous fiber). Approximately 2 hours before the emergence of the DTS spike, low-frequency (1 Hz) strain-rate data recorded using Distributed Acoustic Sensing (DAS) fiber captured an extensional signal at this same depth (Figure 6). This strain-rate perturbation persists until injection is stopped on 17 August. Upon stopping injection, the extensional signal rapidly becomes contractional and then disappears shortly thereafter. Furthermore, observers in the drift noted that AML started producing a milky white liquid dripping from the collar after this shut-in test was initiated (Figure 7). Observers also saw more water flowing into the drift in general during this test.

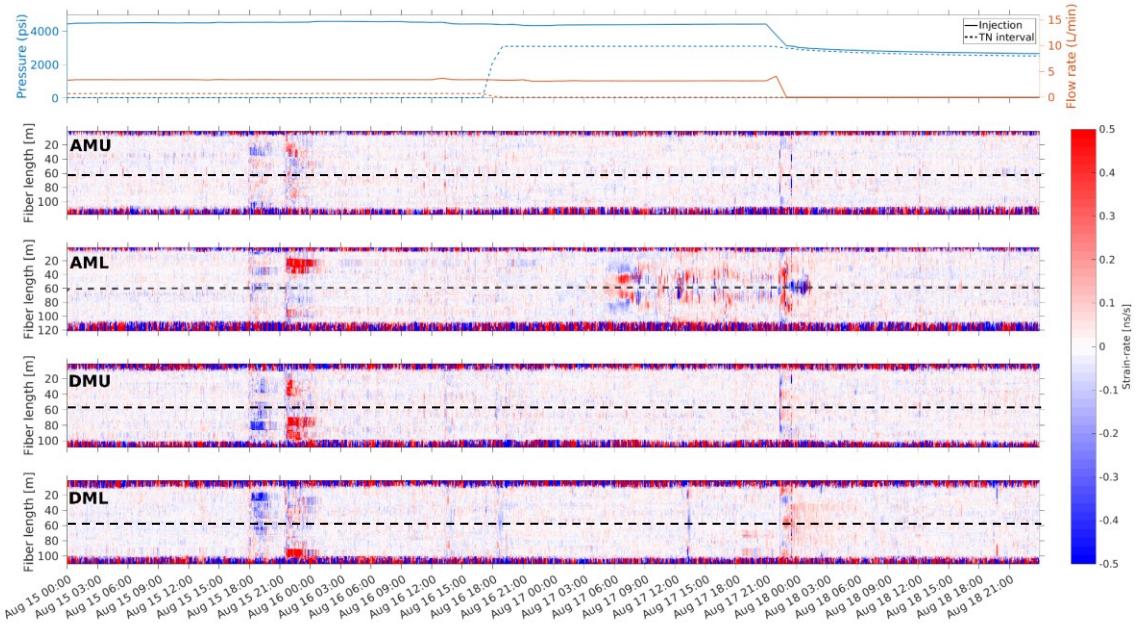

Figure 6: "Waterfall" color plot showing low-frequency (1 Hz) strain-rate recorded by the continuous DAS fiber in the four grouted monitoring wells AMU, AML, DMU, and DML during shut-in testing. Red/positive strain indicates extension, blue/negative strain indicates compression. Flow/pressure values for TU (injection) and TN are shown for reference in the top panel. Dashed line indicates the bottom of each well. A strain-rate perturbation is visible at a depth of 40-50 m in borehole AML, coinciding with the DTS spike of Figure 5.

This portion of shut-in testing was intended to be conducted using a constant injection rate in the TU interval. Shortly after the second three-zone shut-in test, however, the injection rate had to be reduced from 3.4 to 3.0 L/min due to destabilization of the pump's pressure/flow performance (Figure 4). This destabilization was associated with mechanical fatigue of the injection pump, following later inspection of the equipment upon completion of the experiment. A slight decrease in TC collar outflow aligns with this injection rate reduction (Figure 4).

Figure 7: Milky fluid leaking from the AML collar observed on 17 August 2022.

3.4 Injection Interval Shut-In Test

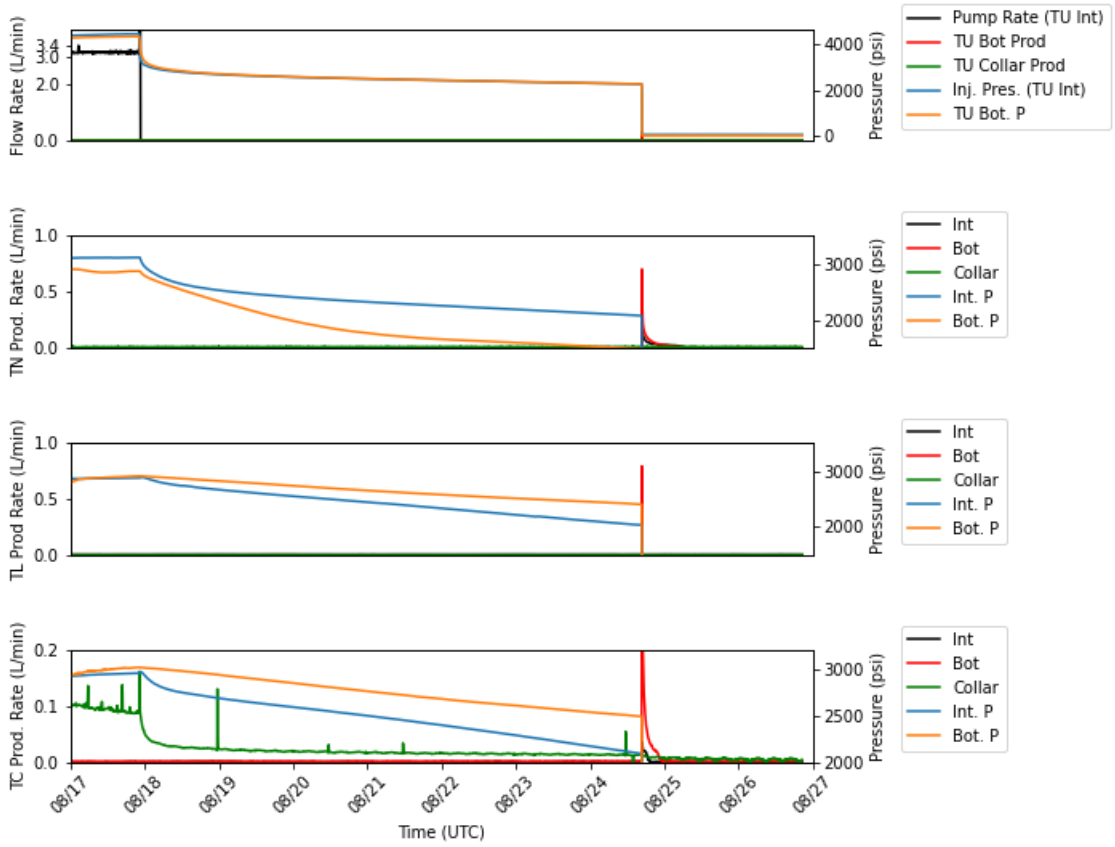

Figure 8: Injection stopped to commence a week-long shut-in test of all 8 zones followed by opening all zones.

Near the end of 17 August 2022, injection was stopped to perform a shut-in test of the TU packer interval and commenced a week-long shut-in test of all eight packer intervals and bottom injection/production zones (Figure 8). The TU packer interval (injection interval) and bottom zones behaved similarly, settling towards a pressure of approximately 17.2 MPa (2,500 psi). The other six production zones exhibited various

behaviors 1) upon initiation of this shut-in test and 2) over the course of the shut-in test. These observations are examined in more detail and interpreted in the interpretation section below.

The start of this shut-in test is correlated with the disappearance of a thermal DTS spike in grouted monitoring well DML (Figure 9). The spike first appeared at a depth of approximately 25 meters (appears again in the return portion of the fiber at approximately 90 meters) following an unplanned injection perturbation during the circulation test that occurred on 19 July 2022 (Figure 9). After the one-week duration, the test was concluded by opening all eight zones to atmospheric pressure (Figure 8). The DTS spike in AML persisted throughout the week-long shut-in test but disappeared after the zones were opened (Figures 5 & 9). After injection was stopped, no distinguishable strain signal was captured by the DAS system (Figure 6). Observers noted that outflow in the 4100L drift decreased rapidly after injection stopped, which was fully anticipated.

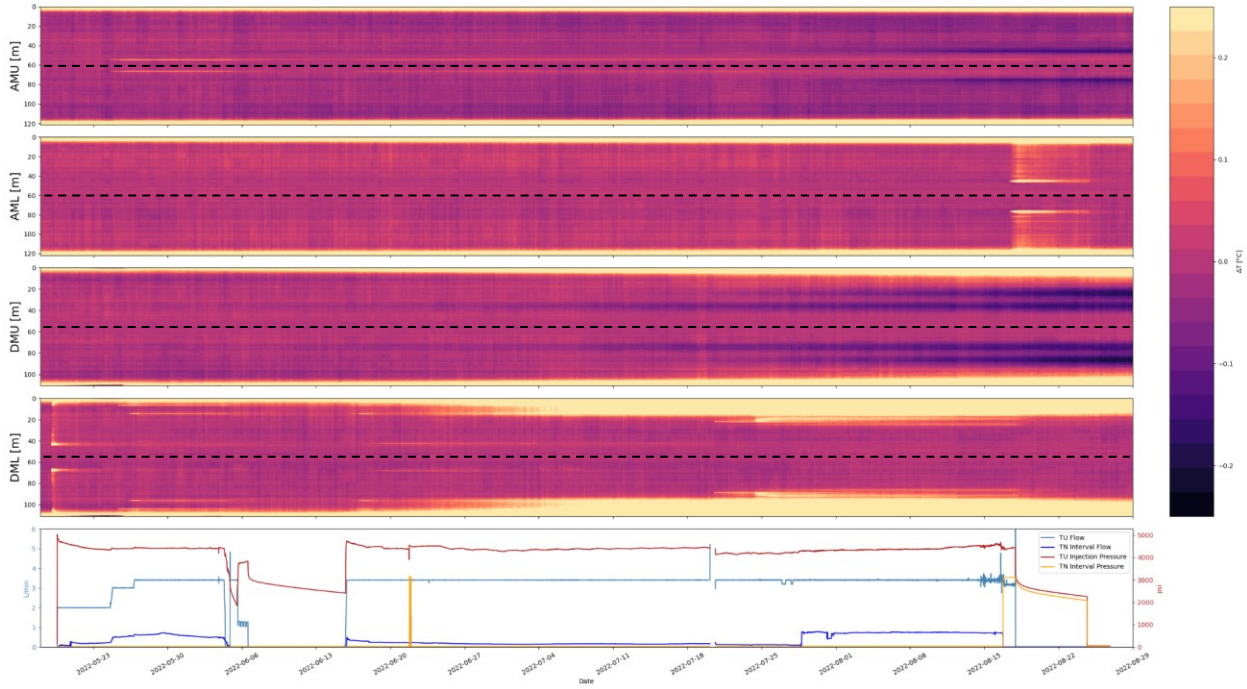

Figure 9: "Waterfall" color plot showing changes in temperature detected by the DTS during circulation and shut-in testing. Dashed line indicates the bottom of each well. The time and color saturation scales highlight the DML temperature spike at approximately 25 meters that disappears after injection stops. The AML spike (see also Figure 5) persists until all zones are opened to atmospheric pressure.

4. INTERPRETATION AND DISCUSSION

Figure 10 shows the results of each shut-in test, over a 20-hour duration, that occurred during injection for direct comparison and analysis of ISIP. The shut-in test for the bottom zone of TU indicates there was direct pressure communication with the injection interval (i.e., a pressure bypass of the lower straddle packer). The other zones converge towards an ISIP of approximately 20 MPa (2,900 psi), within the range of the ISIP values for TV4100 albeit at the low end (Ingraham et al., 2020). The curves indicate closure after shut-in, suggesting no residual permeability (e.g., from shearing) as also determined from Experiment 2. These ISIP values and behaviors do vary, however, among the production zones. The bottom zones have a larger borehole volume than the interval zones, and thus the bottom zone shut-in pressures generally take longer to stabilize than the interval zones. The most extreme case of this behavior is the TL bottom zone, which suggests a lack of hydraulic connectivity with the injection zone. On the other end of the spectrum is the TN bottom zone, which has the most robust/direct connection to the injection zone of the bottom zones (i.e., highest bottom zone outflow recovery during circulation testing). The TN interval has the highest ISIP of the production zones at approximately 21.4 MPa (3,100 psi). This is likely the result of hydraulic connectivity to the injection zone, as the TN interval was the highest-producing outflow zone among these wells during circulation testing. Connectivity with the injection interval also most likely explains why the TC interval shut-in pressure simultaneously increases while the TU injection interval pressure increases after increasing the injection temperature (Figure 2). The pressure increase accompanied by increasing injection temperature appears to be a thermo-mechanical skin effect in which the temperature of the injected fluid changes the near-wellbore flow resistance (White & Burghardt, 2021). By increasing the injection temperature, the viscosity of the injected fluid is reduced and likely increases the average viscosity along the fracture path. This may result in the observed elevated pressure responses in the TC and TU intervals.

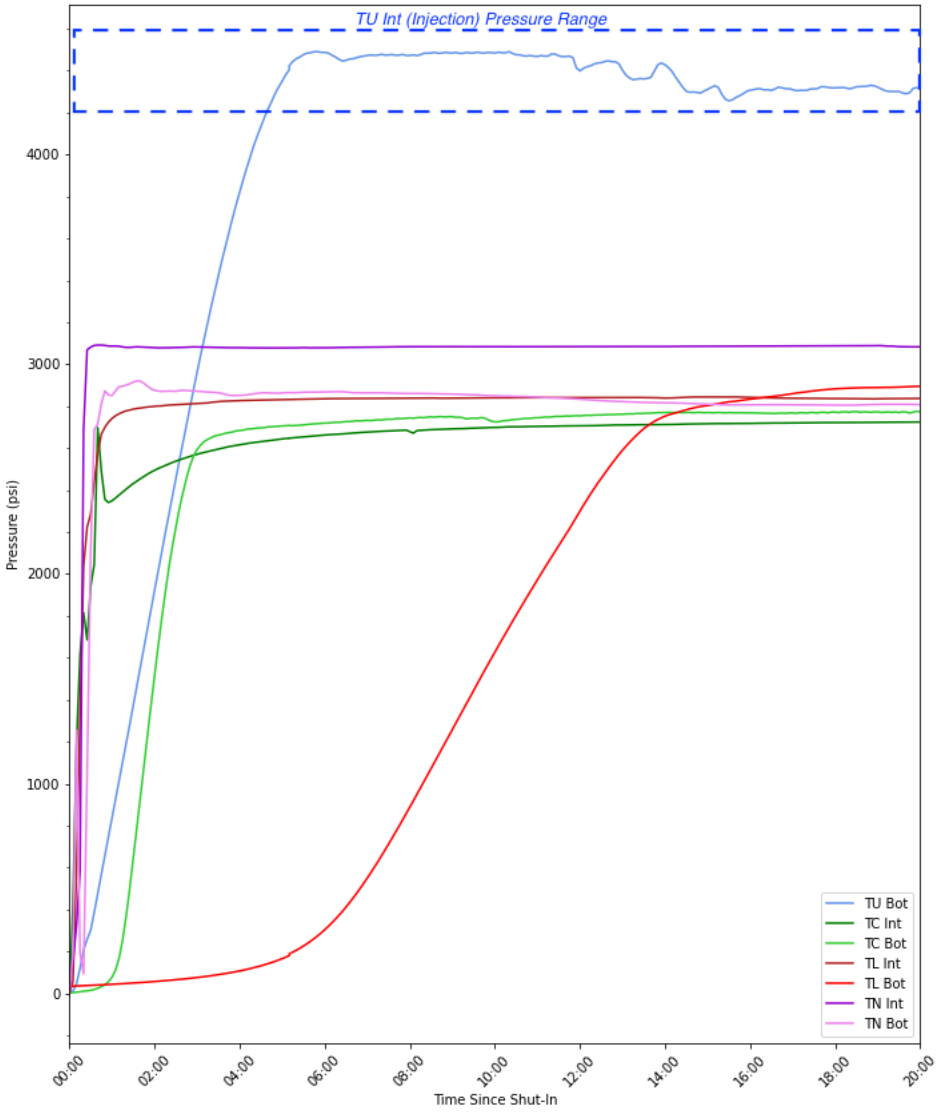

Figure 10: Stack plot showing a 20-hour duration of all seven production zones shut-in tests conducted during injection.

The shut-in test of TN, the highest producing well up to that point, appears to have induced fracture opening and redirection of outflow. A particular instance of this was captured in AML. The DAS in AML, at a depth of approximately 45 meters, indicates fracture opening (extensional) signal after shut-in of TN (Figure 6). This is followed by a DTS signal spike that indicates subsequent inflow of fluid into the grouted borehole at the same depth (Figure 5). The fluid appears to have migrated up the grouted borehole, likely along a channelized pathway in the grout, and expressed as milky white liquid (i.e., water containing grout particles) leaking out of the AML collar as seen in Figure 7. Outflow increases observed in the drift during this time frame further suggest that fractures/fluid migrated to additional hydraulic pathways after the shut-in of the TN production zones.

Figure 11 shows the pressure responses of all 7 production zones following shut-in of the TU injection zone, which is also plotted, for a week-long full system shut-in test. The pressure in each zone gradually decreases until the test is concluded by opening all zones to atmospheric pressure. Rapid near-wellbore losses from the injection well are indicated by the initial decline in the injection well pressure compared to the lower production zone pressure magnitudes and rates of decline. As with the shut-in tests during injection, these results generally show more gradual pressure decline curves in the larger-volume bottom zones than the interval zones. The TN bottom zone has the largest pressure loss, which is likely related to this zone's proximity to the highest-outflow zone observed in the 4100L drift near the Battery Alcove (Mattson et al., 2023). That is, the TN bottom zone likely has the most robust hydraulic connection to this high-leakoff pathway to the drift. The TC and TL bottom zones as well as the TL interval zones have gradual pressure declines, suggesting these zones are hydraulically isolated. The relatively rapid, early pressure decline of the TN and TC production intervals indicate initial connection with the injection interval. The pressure in these two zones then overtake and diverge from the injection pressure decline within 24 hours of the shut-in of the injection interval, suggesting that the zones became disconnected/isolated from the injection zone.

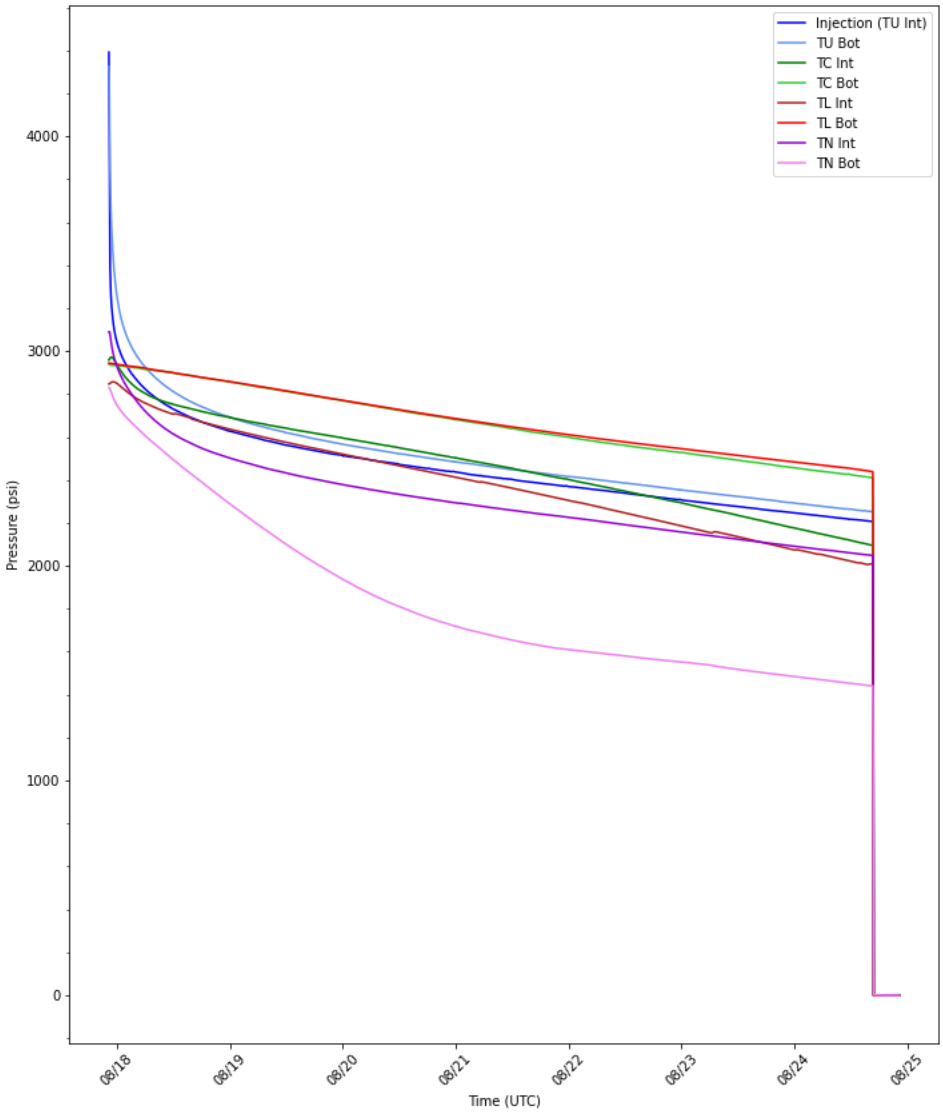

Figure 11: Stack plot showing one-week duration of shut-in test for all eight zones after injection was stopped.

The cessation of injection and the subsequent opening of the test wells to atmospheric pressure each resulted in fracture/hydrological changes in the testbed. While these changes were generally anticipated, for instance the expected and observed rapid decline of outflow in the drift, the distributed fiber monitoring systems added valuable insights on the timing and nature of these effects. After injection stopped, Figure 9 shows that the DTS spike at a depth of 25 meters in DML (which had persisted for a month) disappeared. This suggests a post-injection fracture closure that stopped outflow into DML. The DAS signal in AML reverses from extensional to compressional after injection stops (Figure 6), however the associated DTS spike does not disappear into the background until after the wells are opened (Figure 5). The DAS compressional signal in AML appears to be more closely related to the shut-in rather than stopping injection, indicating a robust fracture connection (previously generated by the shut-in of TN) between the TU injection interval and AML. Once the wells were opened to atmospheric pressure, the subsequent disappearance of the DTS spike in AML indicates this fracture closes and disconnects the hydraulic pathway between AML and the TU injection interval.

These shut-in tests inform the evolving conceptual understanding of the state of stress and the dynamic influence of fractures in the Experiment 2/3 testbed. The combination of stimulation, circulation, and shut-in tests reveal that, despite being different by only a few degrees in trajectory and thus only having a borehole separation on the scale of meters where stimulations were conducted (Table 1, Figure 1), there are considerable differences in the stress conditions and fracture networks of wells TU and TC. TU formed more robust hydraulic fracture connections with the surrounding test wells than TC (Table 3), but TU exhibits high pressure losses that appear to be related to near-wellbore skin effects (Figure 11). TC, despite its central location, appears to be relatively isolated with respect to the surrounding wells and does not seem to have such a strong skin effect. Conceptually, the differences between TU and TC and the shut-in tests of all four wells during injection suggest that TU produced a hydraulic 'pressure bubble' around the injection interval. Heterogeneity of responses during injection indicate that the 'bubble' had complex and varying connections to the production zones (Figure 10). These ISIP responses during and after injection may be related directly to stress heterogeneity and/or variations in fracture toughness and viscosity of circulating fluid.

There are parallels between these findings from the Experiment 2/3 testbed and those of the kISMET / Experiment 1 testbeds that are relevant to crystalline rock EGS development. Despite being established at different depths and hosted in different geologic formations, the testbeds are broadly characterized by significant geological and geomechanical heterogeneities encountered and measured in wells drilled more vertically compared to wells drilled more horizontally (e.g., Oldenburg et al., 2017; Kneafsey et al., 2020; Ingraham et al., 2020; Burghardt et al., 2022). Stress measurements and shut-in test results appear to be substantially biased by anisotropy in geologic composition and structural fabric that constitute the complex and dynamic nature of near-wellbore skin effects, hydraulic connectivity, and fracture propagation/closure observed in these testbeds. These characteristics similarly impacted the evolution and results of stimulation/circulation testing in both testbeds. In summary, the whole body of mesoscale research conducted in these testbeds at SURF suggests that anisotropy/heterogeneity in lithology, stress, and structure will have significant impacts on EGS applications in crystalline rocks.

5. CONCLUSION AND IMPLICATIONS

The goal of the EGS Collab project was to collect a comprehensive dataset of observations from a crystalline rock mass undergoing mesoscale fracture stimulation and thermal water circulation. The use of an underground test facility at low temperature allows a much more comprehensive monitoring network both in terms of the methods employed and the three-dimensional deployment within and around the stimulated rock volume to an extent not possible in a full-scale geothermal system at reservoir depth. These data are being made available on the Geothermal Data Repository (https://gdr.openei.org/).

The EGS Collab team established two testbeds at SURF. The first testbed hosted Experiment 1, in the 4850L drift, which was focused on hydraulic fracturing research. The second testbed was established in the 4100L drift for Experiment 2, which was focused on shear stimulation research. The shear stimulation experiments did not yield sustained fracture aperture (i.e., enhanced permeability) after injection pressure was removed. That is, as with Experiment 1 in the 4850L drift, significant circulation between production and injection boreholes could only be achieved at injection pressures well above the minimum principal stress determined from hydraulic fracturing stress measurements. The project thus transitioned to Experiment 3 hydraulic stimulation experiments to develop a suitable fracture network for conducting thermal circulation testing. These stimulation experiments ultimately resulted in choosing a well that was intended for monitoring/production (TU) to replace the well originally intended for injection (TC).

For the Experiment 2 circulation, the injection pressure exceeded 30 MPa and thus was well above the 20-23 MPa of ISIP from hydraulic fracturing stress measurements. Due to near-wellbore skin effects, the injection pressure represents the high end of pressures within the stimulated fracture network. The pressures in the fracture network farther from the injection point can be expected to vary depending on the inflation of fractures at pressures above the minimum stress, opening of fractures due to shear stimulation below the minimum stress value, and leakage to sinks at atmospheric pressure such as open sections of boreholes and the mine drift. During the circulation experiment, all borehole intervals were open to mine air pressure and served as production boreholes. Thus, the only measurement of pressure in the stimulated fracture network was at the injection interval. Shut-in tests provided information on the pressure in the stimulated volume, though these have some limitations in that the sections of borehole above the packers and the mine openings remained at atmospheric pressure and continued to serve as sinks.

The shut-in pressure data has not yet been subjected to a rigorous pressure-transient analysis to assess fracture closure and the overall deflation of the stimulated fracture network. Additional data from other geophysical monitoring tools (e.g., microseismicity and electrical resistivity tomography), which have not yet been fully processed and analyzed for the shut-in testing period, will likely offer additional details and refinements to interpretation. Nonetheless, some general conclusions can be drawn from the data and observations:

1. ISIP values generally are consistent with minimum stress estimates obtained from a nearby borehole (TV4100).
2. The immediate drop in pressure in the TU injection interval indicates that there is significant (i.e., 3-10 MPa) near-borehole impedance to flow and the injection pressure was considerably higher than the pressure in the stimulated fracture network. The bottom zone of TU, below the injection interval, is well-connected to the injection interval.
3. The longer duration pressure decline of other zones reflects connectivity to pressure sinks. In particular, the TN bottom interval has the strongest pressure decline, and that interval is interpreted to have strong connections to the mine openings from observations of water outflow in the 4100L drift as well as rapid arrival of tracers during transport experiments.
4. The lack of significant circulation between injection and production wells, at pressures below the minimum stress value, suggest that the initial circulation and the establishment of connections from TU to the main producing intervals in TC and TN did not benefit from shear stimulation below the minimum stress value. It is possible, however, that shear stimulation may have occurred subsequently as the stimulated fracture network expanded during the long-term stimulated circulation. Further analysis of the deflation of the stimulated volume from the shut-in pressure data may shed light on a) where fractures are closing during the deflation, b) how these closures reflect the complex fracture network geometry, and c) the role of hydromechanical coupling.

These results have implications applicable to EGS Collab objectives and more broadly to crystalline rock / EGS research. The shut-in tests provide important model input parameters for calibration and validation of intermediate-scale EGS Collab models. The inter-well and fracture network interactions captured by this suite of well-monitored shut-in tests demonstrate that the system as a whole is heterogeneous and complexly linked, which has significant impacts on ISIP values/behaviors and the relationship to the minimum principal stress. It is reasonable to expect that similar complex conditions may be encountered in other crystalline rock masses. For full-scale EGS applications, these conditions will similarly need to be modeled and characterized to assure sustainable fracture permeability and thermal circulation.

ACKNOWLEDGEMENTS

This material was based upon work supported by the U.S. Department of Energy, Office of Energy Efficiency and Renewable Energy (EERE), Office of Technology Development, Geothermal Technologies Office, under Award Number DE-NA0003525 with Sandia National Laboratories and other awards to other national laboratories. The United States Government retains, and the publisher, by accepting the article for publication, acknowledges that the United States Government retains a non-exclusive, paid-up, irrevocable, world-wide license to publish or reproduce the published form of this manuscript, or allow others to do so, for United States Government purposes. Sandia National Laboratories is a multimission laboratory managed and operated by National Technology & Engineering Solutions of Sandia, LLC, a wholly owned subsidiary of Honeywell International Inc., for the U.S. Department of Energy's National Nuclear Security Administration under contract DE-NA0003525. Portions of this work were performed under the auspices of the U.S. Department of Energy by Lawrence Livermore National Laboratory under Contract DE-AC52-07NA27344. This paper describes objective technical results and analysis. Any subjective views or opinions that might be expressed in the paper do not necessarily represent the views of the U.S. Department of Energy or the United States Government. The research supporting this work took place in whole or in part at the Sanford Underground Research Facility in Lead, South Dakota. The assistance of the Sanford Underground Research Facility and its personnel in providing physical access and general logistical and technical support is gratefully acknowledged. We also thank the crew from RESPEC, who logged the core upon recovery from drilling, and also supported the wireline logging operations. The earth model output for this paper was generated using Leapfrog Software, copyright Seequent Limited. Leapfrog and all other Seequent Limited product or service names are registered trademarks or trademarks of Seequent Limited.

REFERENCES

Burghardt, J., Doe, T., Ingraham, M., Schwering, P., Ulrich, C., Roggenthen, W.M., Reimers, C., & EGS Collab Team: Integration of Shut-In Pressure Decline, Flow back, Hydraulic and Sleeve Re-Opening Tests to Infer In-Situ Stress, Proceedings, 54th US Rock Mechanics/Geomechanics Symposium, Golden, CO (2020).

Burghardt, J., Knox, H.A., Doe, T., Blankenship, D., Schwering, P., Ingraham, M., Kneafsey, T.J., Dobson, P.F., Ulrich, C., Guglielmi, Y., & Roggenthen, W.: EGS Stimulation Design with Uncertainty Quantification at the EGS Collab Site, Proceedings, 56th US Rock Mechanics/Geomechanics Symposium, Santa Fe, NM (2022).

Dobson, P., Kneafsey, T., Morris, J., Singh, A., Zoback, M., Roggenthen, W., Doe, T., Neupane, G., Podgorney, R., Wang, H., Knox, H., Schwering, P., Blankenship, D., Ulrich, C., Johnson, T., White, M., & EGS Collab Team: The EGS Collab Hydroshear Experiment at the Sanford Underground Research Facility – Siting Criteria and Evaluation of Candidate Sites, Geothermal Resources Council Transactions, Vol. 42 (2018).

Guglielmi, Y., Cappa, F., Avouac, J.P., Henry, P., & Elsworth, D.: Seismicity Triggered by Fluid Injection–Induced Aseismic Slip, Science, 348(6240), 1224 (2015).

Guglielmi, Y., Cook, P., Soom, F., Dobson, P., Kneafsey, T., Valley, B., Kakurina, M., Niemi, A., Tsang, C.F., Tatomir, A., Juhlin, C., & Basirat, F.: Estimating Stress from Three-Dimensional Borehole Displacements Induced by Fluid Injection in Different Types of Fractured or Faulted Rocks, Proceedings, 55th US Rock Mechanics/Geomechanics Symposium, Houston, TX (2021a).

Guglielmi, Y., Cook, P., Soom, F., Schoenball, M., Dobson, P., & Kneafsey, T.: In Situ Continuous Monitoring of Borehole Displacements Induced by Stimulated Hydrofracture Growth, Geophysical Research Letters, 48, https://doi.org/10.1029/2020GL090782 (2021b).

Guglielmi, Y., Cappa, F., Rutqvist, J., Tsang, C.F., Wang, J., Lançon, H., Durand, J., & Janowczyk, J.B.: Step-Rate Injection Method for Fracture In-Situ Properties (SIMFIP): Monitoring Fractures Stimulation Efficiency, Proceedings, 48th U.S. Rock Mechanics/Geomechanics Symposium, Minneapolis, MN (2014).

Heise, J.: The Sanford Underground Research Facility at Homestake, Journal of Physics: Conference Series, 606(1), 26 (2015).

Ingraham, M.D., Schwering, P.C., Burghardt, J., Ulrich, C., Doe, T., Roggenthen, W.M., & Reimers, C.: Analysis of Hydraulic Fracturing on the 4100 Level at the Sanford Underground Research Facility, Proceedings, 54th US Rock Mechanics/Geomechanics Symposium, Golden, CO (2020).

Ingraham, M., Strickland, C., Vermeul, V., Roberts, B., Burghardt, J., Schwering, P., Knox, H., & EGS Collab Team: Design and Fabrication of a Remote-Control Hydraulic Fracturing System, Geothermal Resources Council Transactions, Vol. 45 (2021).

Kneafsey, T., Blankenship, D., Dobson, P., Burghardt, J., White, M., Morris, J.P., Johnson, T., Ingraham, M., Ulrich, C., Roggenthen, W., Doe, T., Smith, M., Ajo-Franklin, J.B., Huang, L., Neupane, G., Pyatina, T., Schwering, P.C., Hopp, C., Rodríguez Tribaldos, V., Guglielmi, Y., Strickland, C., Vermeul, V., Fu, P., Knox, H.A., & EGS Collab Team: The EGS Collab – Initial Results from Experiment 2: Shear Stimulation at 1.25 km Depth, Proceedings, 47th Workshop on Geothermal Reservoir Engineering, Stanford University, Stanford, CA (2022a).

Kneafsey, T., Blankenship, D., Dobson, P., Morris, J., White, M., Fu, P., Schwering, P., Ajo-Franklin, J., Huang, L., Schoenball, M., Johnson, T., Knox, H., Neupane, G., Weers, J., Horne, R., Zhang, Y., Roggenthen, W., Doe, T., Mattson, E., Valladao, C., & EGS Collab Team: The EGS Collab Project: Learnings from Experiment 1, Proceedings, 45th Workshop on Geothermal Reservoir Engineering, Stanford University, Stanford, CA (2020).

Kneafsey, T.J., Dobson, P.F., Ulrich, C., Hopp, C., Rodríguez Tribaldos, V., Guglielmi, Y., Blankenship, D., Schwering, P.C., Ingraham, M., Burghardt, J.A., White, M.D., Johnson, T.C., Strickland, C., Vermeul, V., Knox, H.A., Morris, J.P., Fu, P., Smith, M., Wu, H., Ajo-

Franklin, J.B., Huang, L., Neupane, G., Horne, R., Roggenthen, W., Weers, J., Doe, T.W., & EGS Collab Team: The EGS Collab Project – Stimulations at Two Depths, Proceedings, 56th US Rock Mechanics/Geomechanics Symposium, Santa Fe, NM (2022b).

Kneafsey, T., Blankenship, D., Burghardt, J., Johnson, T., Dobson, P., Schwering, P.C., Hopp, C., White, M., Morris, J.P., Strickland, C., Vermeul, V., Fu, P., Ingraham, M., Roggenthen, W., Doe, T., Ajo-Franklin, J.B., Huang, L., Rodríguez Tribaldos, V., Guglielmi, Y., Knox, H., Cook, P., Soom, F., Ulrich, C., Frash, L. Neupane, G., Pyatina, T., Weers, J., Mattson, E., Robertson, M., & EGS Collab Team: The EGS Collab - Discoveries and Lessons from an Underground Experiment Series, Proceedings, 48th Workshop on Geothermal Reservoir Engineering, Stanford University, Stanford, CA (2023).

Mattson, E.D., Neupane, G., White, M.D., & Ingraham, M.D.: EGS-Collab Experiment 1 Flow and Tracer Tests at the Sanford Underground Research Facility, Proceedings, 55th US Rock Mechanics/Geomechanics Symposium, Houston, TX (2021).

Mattson, E., Plummer, M., Neupane, H., Vermeul, V., Sirota, D., Ingraham, M., Kneafsey, T., & EGS Collab Team: Fluorescein Tracer Testing on the 4100L – A Preliminary Examination of Initial Arrival in Wells and the Drift at the Second EGS Collab Testbed, Proceedings, 48th Workshop on Geothermal Reservoir Engineering, Stanford University, Stanford, CA (2023).

Meng, M., Frash, L.P., Li, W., Welch, N.J., & Carey, J.W.: Measurement of Geomechanical and Hydrological Properties of EGS-Collab Geothermal Rocks, Proceedings, 55th US Rock Mechanics/Geomechanics Symposium, Houston, TX (2021).

Meng, M., Frash, L.P., Li, W., Welch, N.J., Carey, J.W., Morris, J., Neupane, G., Ulrich, C., & Kneafsey, T.: Hydro-Mechanical Measurements of Sheared Crystalline Rock Fractures With Applications for EGS Collab Experiments 1 and 2, Journal of Geophysical Research: Solid Earth, 127(2), e2021JB023000, https://doi.org/10.1029/2021JB023000 (2022).

Neupane, G., Mattson, E.D., Plummer, M.A., Podgorney, R.K., & EGS Collab Team: Results of Multiple Tracer Injections into Fractures in the EGS Collab Testbed-1, Proceedings, 45th Workshop on Geothermal Reservoir Engineering, Stanford University, Stanford, CA (2020).

Oldenburg, C.M., Dobson, P.F., Wu, Y., Cook, P.J., Kneafsey, T.J., Nakagawa, S., Ulrich, C., Siler, D.L., Guglielmi, Y., Ajo-Franklin, J., Rutqvist, J., Daley, T.M., Birkholzer, J.T., Wang, H.F., Lord, N.E., Haimson, B.C., Sone, H., Vigilante, P., Roggenthen, W.M., Doe, T.W., Lee, M.Y., Ingraham, M., Huang, H., Mattson, E.D., Zhou, J., Johnson, T.J., Zoback, M.D., Morris, J.P., White, J.A., Johnson, P.A., Coblentz, D.D., & Heise, J.: Overview of the kISMET Project on Intermediate-Scale Hydraulic Fracturing in a Deep Mine, Proceedings, 51st US Rock Mechanics/Geomechanics Symposium, San Francisco, CA (2017).

Singh, A., Zoback, M., Dobson, P.F., Kneafsey, T.J., Schoenball, M., Guglielmi, Y., Ulrich, C., Roggenthen, W., Uzunlar, N., Morris, J., Fu, P., Schwering, P.C., Knox, H.A., Frash, L., Doe, T.W., Wang, H., Condon, K., Johnston, B., & EGS Collab Team: Slip Tendency Analysis of Fracture Networks to Determine Suitability of Candidate Testbeds for the EGS Collab Hydroshear Experiment, Geothermal Resources Council Transactions, Vol. 43 (2019).

White, M.D. & Burghardt, J.A.: Modeling the Dynamic Flow Resistance Across the Fracture Network of EGS Collab Experiment 1, Proceedings, 46th Workshop on Geothermal Reservoir Engineering, Stanford University, Stanford, CA (2021).